



“Gheorghe Asachi” Technical University of Iasi, Romania



## EVALUATION OF COPPER AND LEAD BIOSORPTION ON MODIFIED *Azolla pinnata* (R. Br.)

Arielle Barros\*, Sirlei Kleinübing Meuris da Silva

Chemical Engineering Faculty of the University of Campinas, Av. Albert Einstein 500, postcode: 13083-852, Campinas, Brazil

### Abstract

This paper investigates the macrophyte *Azolla pinnata* modified with sodium hydroxide, as a bioadsorbent for  $\text{Cu}^{2+}$  and  $\text{Pb}^{2+}$  ions in synthetic solutions. Biomaterial characterization was performed using Scanning Electronic Microscopy (SEM); Energy-Dispersive X-Ray Spectroscopy (EDX); Fourier Transform Infra-red (FTIR) spectroscopy techniques and through the blocking of carboxylic and sulfonic functional groups. Kinetics of the process has highlighted a quick and efficient adsorption, even in low ion concentrations. Langmuir isotherm fitted well the biosorption equilibrium, and the maximum  $\text{Cu}^{2+}$  and  $\text{Pb}^{2+}$  uptake capacities were  $0.448$  and  $0.472 \text{ mmol g}^{-1}$  at  $25^\circ\text{C}$  and  $0.474$  and  $0.614 \text{ mmol g}^{-1}$  at  $45^\circ\text{C}$ , respectively. Desorption process was evaluated using different eluents and calcium chloride has presented the best desorption efficiency, moreover, did not cause visual damage to the material or decreased the adsorption capacity of the biomass.

**Keywords:** biosorption, desorption, heavy metal, macrophyte

Received: May, 2013; Revised final: May, 2014; Accepted: May, 2014; Published in final edited form: January 2018

### 1. Introduction

Heavy metals are species that can be very toxic to any form of life and as they are not biodegradable, they can accumulate in the environment. Lead is mainly used in processes such as manufacturing of batteries, ammunitions and coating. Copper is broadly used in the production of metallic alloys and conducting materials (Puranik and Paknikar, 1997).

The most commonly used techniques for treating effluents with heavy metals include chemical precipitation, ionic exchange, evaporation and reverse osmosis. However, these technologies are usually expensive and/or inefficient when used for removing metallic ions in low concentrations (Jachula et al., 2016; Wilde and Benemann, 1993). Bioadsorption is a specific type of adsorption characterized by the use of materials from biological origin as adsorbents in the removal of a solute. It is an alternative process to conventional treatment methods and, when compared with the existing

metal-removing techniques, its main advantages are the good affinity for metallic ions, low operational cost, minimum volume of chemical and/or biological sludge generated, which will be discarded in landfills after the process, and high efficiency in the detoxification of very diluted effluents (Kratochvil and Volesky, 1998).

Many biomaterials have been evaluated as bioadsorbents for metallic ions such as fungi, bacteria, and more recently, aquatic plants such as algae and macrophytes (Davis et al., 2000; Guibal et al., 1992; Gupta and Rastogi, 2008; Kleinübing et al., 2012, 2011; Manciulea et al., 2017; Sheng et al., 2004).

Among the biomaterials, macrophytes, which are aquatic plants that are well adapted to the weather diversities and present excellent development conditions in sub-tropical climates, have been considered mainly due to their abundance, low cost, ease of growth, capacity of accumulation of some environmental elements where they are inserted and the possibility of reusing biomass, which make its

\* Author to whom all correspondence should be addressed: e-mail: [arielle.mbarros@gmail.com](mailto:arielle.mbarros@gmail.com)

use as bioadsorbent very promising (Lumpkin and Plucknett, 1980; Wagner, 1997).

The capacity of accumulating heavy metals in the aquatic macrophytes has been the reason of the huge interest for treatment of effluents. Cardwell et al. (2002) showed that the concentration of metals in some plants (*Typha* and *Persicaria*) has reached approximately 100,000-fold the value obtained in water. Although *Azolla pinnata* is native to Asia and Africa, the macrophyte is well adapted to the Brazilian climate, since it is developed in tropical and sub-tropical climate. The most favorable temperature to its growth and fixation of nitrogen is between 20-30°C, and only in low as well as very high temperatures (below 5°C and above 45°C) the plant starts dying (Lumpkin and Plucknett, 1980; Wagner, 1997).

*Azolla* main applications are in agriculture as biofertilizer, due to the high rate of nitrogen fixation, providing excellent conditions in organic matter for crops, such as rice, and as animal feed. It can be used to reduce ammonia volatilization from chemical fertilizers and in the control of insects, as well as improving the quality of water, removing the excessive nitrate and phosphorus (Ferentinos et al., 2002; Wagner, 1997). Recently, it has been used in remediation treatment due to several advantages, such as the high production of biomass, simplicity and low cost in cultivation, and the ability of adapting in a wide range of environments (Rai, 2007). There are few studies using *A. pinnata* to remove heavy metal (Arora et al., 2006; Bharti and Banerjee, 2012; Jain et al., 1990), however, they are mainly focused on adsorption capacity and not on process understanding or biomass reuse, leading to a need for further studies.

This paper evaluates modified *Azolla pinnata* biomass as a bioadsorbent for  $\text{Cu}^{2+}$  and  $\text{Pb}^{2+}$  ions and intends to provide better understanding about overall process by studying the parameters related to the characterization of the biomaterial, removal capacity, kinetics and equilibrium of adsorption, process mechanism and also the possibility of recovering and reusing biomass after desorption.

## 2. Experimental

### 2.1. Macrophyte preparation and metal solution

*A. pinnata* seedlings were cultivated in captivity in Brazil. Samples were dried at 55°C overnight and stored. The biomass was ground and sieved and fractions measuring from 0.35 to 0.71 mm were collected for further experiments. In order to be used in the assays, 2g of ground *in-natura* macrophyte was treated with 0.1M sodium hydroxide by placing the biomass in contact with 200 mL NaOH solution for 24h under 200 rpm agitation. After this period, the modified biomass was filtered and rinsed several times with deionized water before being placed in kiln at 55°C for further 24 h. For this study, synthetic solutions of  $\text{Cu}^{2+}$  and  $\text{Pb}^{2+}$  were

prepared from copper and lead nitrate ( $\text{Cu}(\text{NO}_3)_2 \cdot 3\text{H}_2\text{O}$ ,  $\text{Pb}(\text{NO}_3)_2$ ) salts. Ion concentrations were determined by the Atomic Absorption Spectrophotometer (AA 100 – Perkin Elmer).

### 2.2. Surface morphology chemical composition and functional groups

Surface morphology of algae was observed using scanning electron microscope (SEM). After drying, the samples were covered with a thin layer of gold (10 nm) using a sputter coater (SCD 0050 – Baltec, Liechtenstein) and observed using the JEOL JXA-840A scanning electron microscope (20 kV) under vacuum of  $1.33 \times 10^{-6}$  mBar (Jeol, Japan). In order to determine the chemical composition, energy dispersive X-ray spectroscopy was performed on algae after metal adsorption and acidic treatment.

FT-IR spectroscopy was used to confirm the presence of the functional groups in *A. pinnata* samples and observe the chemical modification after heavy metal adsorption in raw and treated biomass. Infrared spectra were recorded in the 4000-650  $\text{cm}^{-1}$  region using a Thermo Nicolet instrument, IR-200 model.

### 2.3. $\text{Cu}^{2+}$ and $\text{Pb}^{2+}$ speciation

Diagrams of  $\text{Cu}^{2+}$  and  $\text{Pb}^{2+}$  species distribution as pH functions were simulated using HYDRA (Hydrochemical Equilibrium-Constant Database) software (Puigdomenech, 2004) to evaluate the best pH value for the experimental runs. The diagrams were made for metal at equilibrium concentration (5  $\text{mmol.L}^{-1}$ ) that corresponded to the maximum copper and lead solutions concentration used in this study.

### 2.4. Blocking of functional groups

Carboxylic and sulfonic groups are considered key functions in biosorption and in order to evaluate their role, they were blocked and removal of copper ion was carried out. Carboxylic groups were esterified according to the work by Gardea-Torresdey et al. (1990), in which 4 g biomass pre-treated with NaOH was placed in 260 mL methanol and 2.4 mL concentrated HCl during 6h under agitation. The biomass was rinsed seven times in batches (10 g/L and 20 min/batch). This biomaterial was submitted to adsorption of copper in pH 4 and 2.

The methodology stated in the study by Fourest and Volesky (1996) was used for blocking sulfonic groups, in which 4 g pre-treated biomass was placed in contact with 260 mL methanol and 2.4 mL HCl and left under agitation for 48 h three times. After every 48h, methanol and acid solution was replaced by a new one. The materials blocked for the sulfonic groups were used in assays in pH 2. In the biomaterial assays with the modified groups, the initial concentration of 0.5 mM in 500 mL copper solution and agitation of 200 rpm at room temperature was used.

## 2.5. Bioadsorption kinetic assays

Bioadsorption kinetic assays in bath system were performed using 500 mL of metallic solution at the concentration of 0.5 mmol L<sup>-1</sup> in contact with 1 g modified macrophyte and agitation of 300 rpm. The pH was kept at 4.5 and adjusted, when necessary, with nitric acid or sodium hydroxide solution. The assays were performed at room temperature (~25 °C). After this, pseudo-first order, pseudo-second order and intra-particle diffusion kinetic models (Eqs. 1-3, respectively) were adjusted to the experimental data obtained.

$$q_t = q_e(1 - e^{-k_1 t}) \quad (1)$$

where  $q_t$  is the concentration of the metallic ion adsorbed in  $t$  minutes [mmol g<sup>-1</sup>];  $t$  is the process time [min];  $q_e$  is the concentration of the metallic ion adsorbed in equilibrium [mmol g<sup>-1</sup>] and;  $k_1$  is the constant in the pseudo-first order absorption rate [h<sup>-1</sup>].

$$q_t = q_e \cdot (q_e \cdot k_2 \cdot t) / [(q_e \cdot k_2 \cdot t) + 1] \quad (2)$$

where  $k_2$  is the constant in the pseudo-second order adsorption rate [g mmol<sup>-1</sup> min<sup>-1</sup>].

$$q_t = k_3 \cdot t^{0.5} \quad (3)$$

where  $k_3$  is the characteristic parameter in the process rate [mmol(g<sup>-1</sup>min<sup>-1/2</sup>)].

## 2.6. Equilibrium assays

In the equilibrium assays, the pre-treated biomass (0.2 g) was placed in contact with 200 mL metallic solutions (Cu<sup>2+</sup> or Pb<sup>2+</sup>) in the following initial concentration values: 0.3, 0.5, 0.7, 1.0, 1.5, 2.0, 3.0, 4.0 and, 5.0 mmol L<sup>-1</sup>, agitation of 300 rpm and pH 4.5. In order to analyze the influence of temperature on the system, assays were performed at 25 and 45°C. The adsorption capacity of metals for each initial concentration was calculated by the equilibrium described by Eq. (4):

$$q_e = [(C_i - C_e) \cdot V] / m \quad (4)$$

where  $q_e$  is the metal concentration in the solution in equilibrium [mmol g<sup>-1</sup>];  $C_e$  is the adsorption capacity of the metal ion in equilibrium [mmol L<sup>-1</sup>];  $C_i$  is the initial concentration of the solution [mmol L<sup>-1</sup>];  $V$  is the initial solution volume [L] and;  $m$  is the modified biomass mass [g].

Langmuir (Eq. 5) and Freundlich (Eq. 6) Isotherm models were adjusted to the experimental data.

$$q_e = (q_{\max} \cdot C_e) / (1/K + C_e) \quad (5)$$

where  $q_{\max}$  is the maximum adsorption capacity in the saturation of the monolayer [mmol g<sup>-1</sup> adsorbent] and;  $K$  is the constant related to the adsorption energy [L mmol<sup>-1</sup>].

$$q_e = K_F \cdot (C_e)^n \quad (6)$$

where  $K_F$  is the constant related to the adsorbent capacity and  $n$  is the constant related to the adsorption intensity.

McCabe et al. (2001) defined the non-dimensional constant  $R_L$  to characterize the type of isotherm calculated by Eq. (7):

$$R_L = 1 / (1 + K \cdot C_o) \quad (7)$$

where  $C_o$  is the highest initial concentration of ions used in this study, i.e., 5 mmol L<sup>-1</sup> [mmol L<sup>-1</sup>]. Thus, it follows that for  $R_L > 1$ , equilibrium is unfavourable; for  $R_L = 1$ , equilibrium is linear; for  $0 < R_L < 1$ , equilibrium is favourable, and for  $R_L = 0$  it is irreversible.

## 2.7. Desorption of ions

Desorption assays were performed under the same agitation and temperature conditions as the bioadsorption assays. Initially, the adsorbent was saturated with 0.5 g macrophyte and placed in contact with 250 mL metallic solution (1 mmol L<sup>-1</sup>) for 3 h. The saturated macrophyte was filtered and placed in kiln at 55 °C for 24 h and, after drying, it was weighed and placed in contact with 250 mL eluent solution. In this paper, three eluents were evaluated: HCl (0.1 M), EDTA (0.05 M) in pH 4.5, and CaCl<sub>2</sub> (0.5 M) in pH 3. After equilibrium, the amount adsorbed was calculated by Eq. (8):

$$q_{el} = (V \cdot C_e) / m_c \quad (8)$$

where,  $q_{el}$  is the amount of eluted metal [mmol g<sup>-1</sup>];  $V$  is the volume of eluent solution [L] and;  $m_c$  is the initial adsorbent mass [g].

Efficiency of desorption was calculated by Eq. (9):

$$efficiency(\%) = C_{ad,1} / C_{de} \quad (9)$$

where,  $C_{ad,1}$  is the concentration of metallic ions at the beginning of the 1<sup>st</sup> adsorption [mmol L<sup>-1</sup>] and  $C_{de}$  is the concentration of metallic ions after desorption [mmol L<sup>-1</sup>].

The biomaterial submitted to desorption was placed in kiln in the same previous conditions, and then, weighted and submitted to a new adsorption cycle. After the 2<sup>nd</sup> adsorption, the percentage of mass lost during one adsorption-desorption-adsorption cycle was calculated.

3. Results and discussion

3.1. Morphology and chemical composition

Fig. 1 presents the results of surface analysis of the macrophyte by scanning electronic microscopy (SEM) and the respective elemental analysis diagrams by EDX. EDX analysis is qualitative and punctual and the percentage value of each element determined might vary depending on the region analyzed. The SEM analyses were performed before and after the adsorption process of metallic ions for a 3000-fold increase. Comparing the image obtained for the *in natura* sample (Fig. 1a), it is possible to notice that it presents greater rugosity than the samples saturated with  $\text{Cu}^{2+}$  (Fig. 1c) and  $\text{Pb}^{2+}$  (Fig.

1e), which shows modifications on the biomaterial surface after adsorption process.

By comparing the EDX results obtained for the *in natura* sample (Fig. 1b) with the samples saturated with  $\text{Cu}^{2+}$  (Fig. 1d) and  $\text{Pb}^{2+}$  (Fig. 1f), it is possible to notice the presence of magnesium (Mg), potassium (K), calcium (Ca) and sodium (Na) in the *in natura* sample and, after the adsorption of metallic ions, these elements disappear. Since these inorganic elements are competing ions, it can be concluded that ionic exchange phenomenon might be involved in the process. As expected, the greatest elemental percentage is that of the adsorbed metal in all cases. In samples saturated with metal, the presence of gold (Au) is due to the use of this material to recover the sample for the SEM analysis.

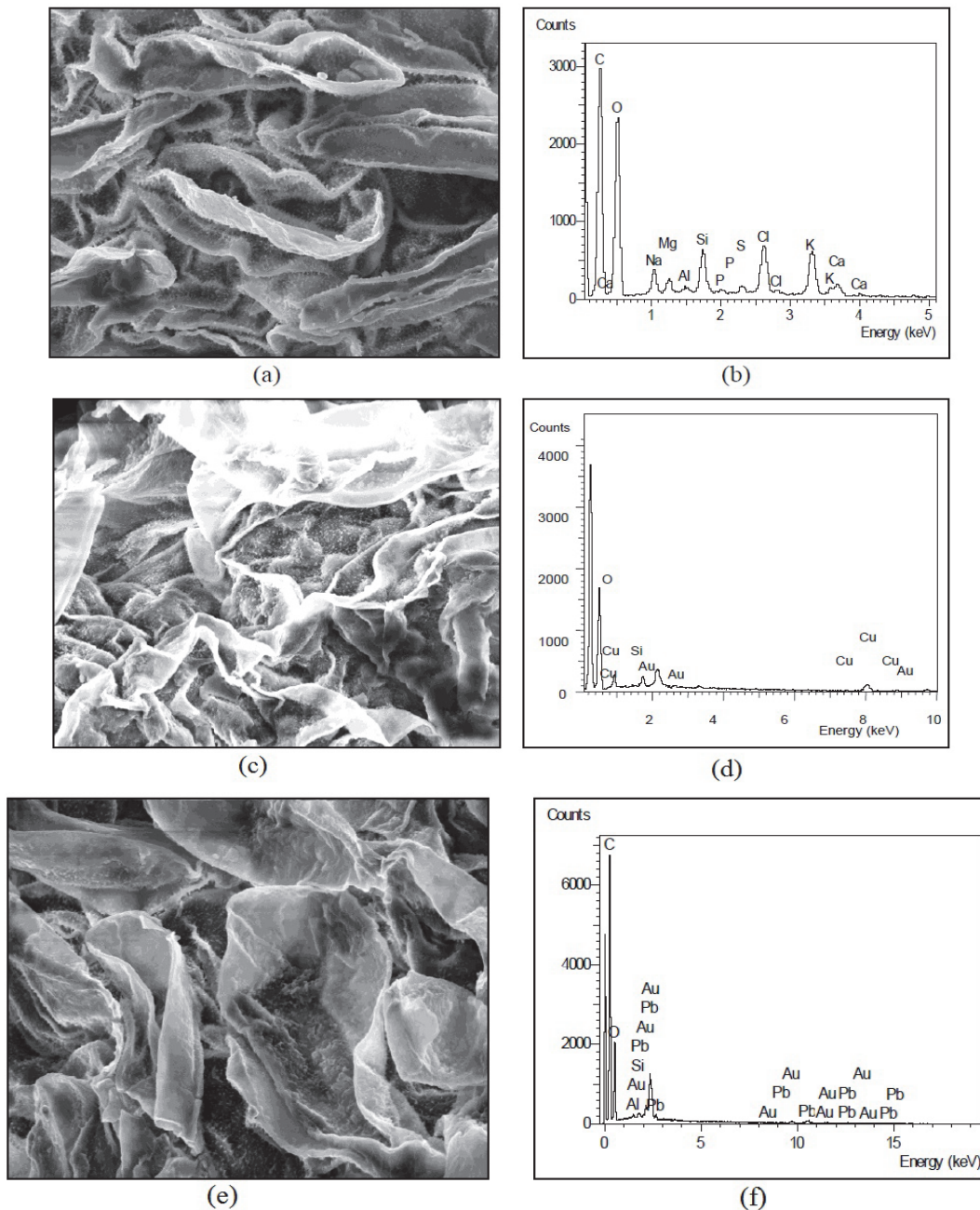


Fig. 1. SEM (a) for *in natura* *A. pinnata* macrophyte and for saturated samples for (c)  $\text{Cu}^{2+}$  and (e)  $\text{Pb}^{2+}$  ions; EDX for (b) *in natura* samples and for saturated samples for (d)  $\text{Cu}^{2+}$  and (f)  $\text{Pb}^{2+}$  ions

### 3.2. Functional groups

Biomaterial surfaces can be regarded as a mosaic of different functional groups that are responsible for binding of metal ions, including amide ( $-\text{NH}_2$ ), carboxylate ( $-\text{COO}^-$ ), thiols ( $-\text{SH}$ ), phosphate ( $\text{PO}_4^{3-}$ ), and hydroxide ( $-\text{OH}$ ). The identification of functional groups is essential for understanding the mechanisms responsible for the binding of certain metal ions (Çelekli et al., 2010; Gupta et al., 2010).

Fig. 2 present the spectra obtained in infra-red region (FTIR) for the *in natura* sample and the sample treated with NaOH. For *in natura* and treated macrophyte, the broad band at  $3000\text{--}3600\text{ cm}^{-1}$  corresponds to the O-H group from cellulose and N-H groups from proteins (Guibaud et al., 2003; Sheng et al., 2004). The  $2923\text{-cm}^{-1}$  band is attributed to vibration of ( $-\text{CH}_2$ ) (Guibaud et al., 2003; Saygideger et al., 2005) and the  $2847\text{-cm}^{-1}$  band is attributed to stretching of (C-H) (Selatnia et al., 2004; Yoonaiwong et al., 2011). The  $1620\text{-cm}^{-1}$  band is attributed to (C-N) and (C=O) stretch of amino groups present in proteins, amides and carboxylic acids (Selatnia et al., 2004). The  $1240\text{-cm}^{-1}$  band is associated to C-O stretch of COOH (Fourest and

Volesky, 1996). The bands at  $1033$ ,  $1095$  and  $1197\text{ cm}^{-1}$  are assigned to the  $-\text{C}-\text{O}$ ,  $-\text{C}-\text{C}$  and  $-\text{C}-\text{OH}$  stretching vibrations (Çelekli et al., 2010; Doshi et al., 2007; Gupta et al., 2010). The adsorption peaks in the region  $900\text{--}750\text{ cm}^{-1}$  could be attributed to  $-\text{P}-\text{O}$ ,  $-\text{S}-\text{O}$ , and aromatic  $-\text{CH}$  stretching vibrations (Çelekli et al., 2010; Gupta et al., 2010).

In Fig. 2a, changes and the appearance of new peaks can be observed after the treatment of biomass with NaOH, with emphasis in the appearance of peak  $1418\text{ cm}^{-1}$ , that may be due to C-OH deformation vibration with contribution of O-C-O symmetric stretching vibration of carboxylate group (Mathlouthi and Koenig, 1987). The treatment could have increased the active sites available for the metallic bonds, probably binding to protons from the functional groups where the modifications can be observed (Fourest and Roux, 1992). Moreover, the reagent did not significantly change the structure of the biomaterial.

Fig. 3 presents the spectra for the samples saturated with  $\text{Cu}^{2+}$  and  $\text{Pb}^{2+}$  metallic ions. The changes after the metal adsorption process can be verified by the comparison with the pre-treated sample.

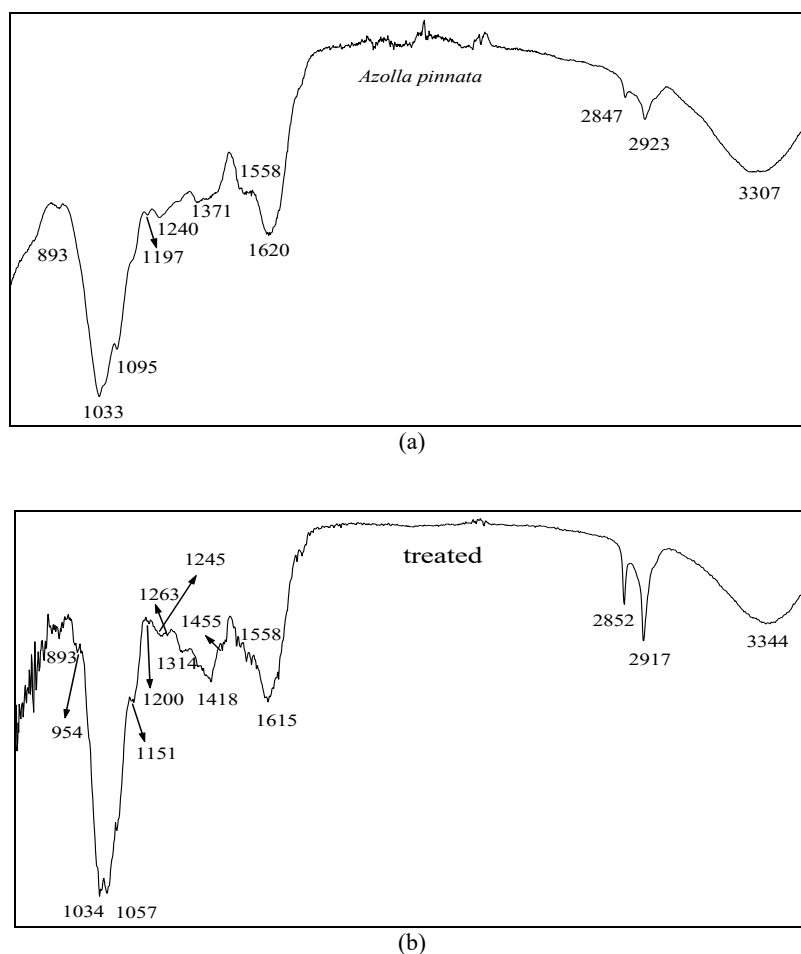


Fig. 2. Spectra obtained for *in natura* (a) and pre-treated with NaOH (b) *A. pinnata*

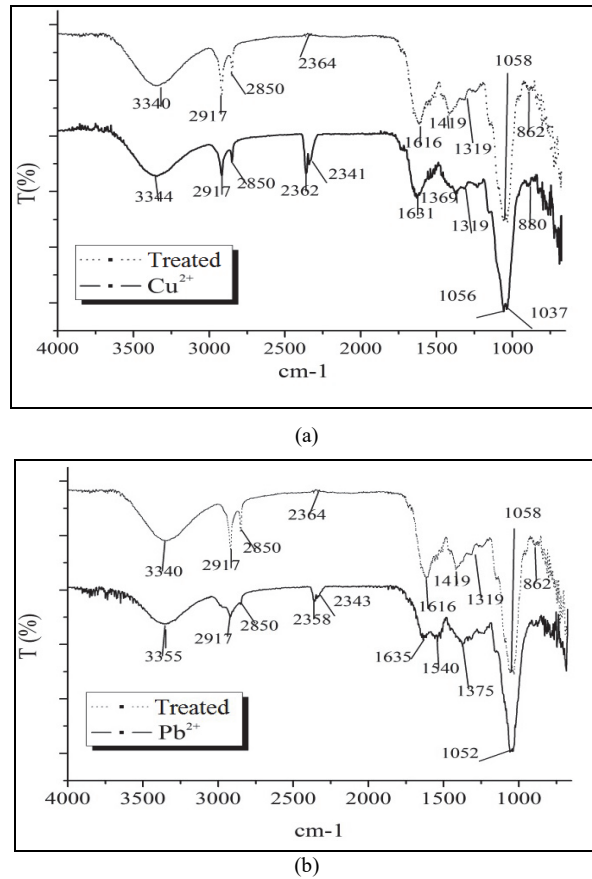


Fig. 3. Comparison of infrared spectrum for treated and saturated *A. pinnata* for (a)  $\text{Cu}^{2+}$  and (b)  $\text{Pb}^{2+}$  ions

The peak at  $1419\text{ cm}^{-1}$  observed in treated macrophyte presents changes after the adsorption of metallic ions. This peak is due to the binding with carboxylate groups (Saygideger et al., 2005). Carboxylates present peaks at approximately  $1630\text{ cm}^{-1}$  (Chen and Yang, 2005) where, by the spectra, alterations can also be observed after the adsorption process. The peaks between  $2250$  and  $2400\text{ cm}^{-1}$  appeared after the adsorption of metals, corresponding to the  $\text{C}=\text{O}$  bindings of aldehydes, ketones and carboxylic acids (Schimmel et al, 2010).

The band at  $1615\text{ cm}^{-1}$  observed in the treated macrophyte was changed after the adsorption of ions and indicate that stretches ( $\text{C}-\text{N}$ ) and ( $\text{C}=\text{O}$ ) from the amino groups present in proteins, amides and carboxylic acids are taking part in the adsorption process. Peaks around  $900-750\text{ cm}^{-1}$  indicate the presence of sulfonated groups. However, these groups are not easily detected. Changes observed in this region indicate these groups might be present and participating in the adsorption process. The analysis of the spectra shows that the main groups modified after the adsorption process were the carboxylates (mainly carboxylic acids), and therefore, this function plays an important role in the adsorption of  $\text{Cu}^{2+}$  and  $\text{Pb}^{2+}$  ions.

### 3.3. Speciation of metals

In order to choose an optimum pH value for this study, the software Hydra (Puigdomenech, 2004)

was used to evaluate species presents in solution according to the pH. Fig. 4 shows the simulation that was performed considering only the solution of metallic ions. In bioadsorption assays, the contact of the bioadsorbent with the solution might alter the system. However, for solubility effects, this simulation might offer a good approximation of the real system.

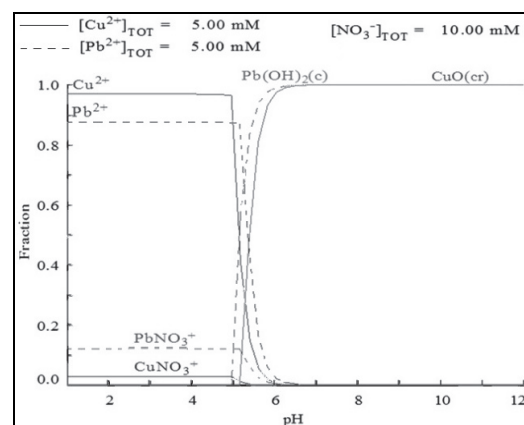


Fig. 4. Speciation for (b)  $\text{Cu}^{2+}$  and (d)  $\text{Pb}^{2+}$  ions

In low pH values (Fig. 4), there is a prevalence of ions in the  $2+$  state. From pH 5, the copper and lead ions start to precipitate. Considering only the pH value that avoids precipitation, each metallic ion could be submitted to adsorption in a different value of pH. However, in order to compare

results between metals, the same pH was defined, that is, 4.5 in all assays and for both metals.

### 3.4. Blocking of functional groups

The bindings between biomaterial-metal can be of several types and carboxylic and sulfonic groups, present in a great variety of biomass, have presented a large contribution in these bindings (Fourest and Volesky, 1996; Sheng et al., 2004). Other groups that might also contribute to the bioadsorption are hydroxyl and proteins. However, the hydroxyl groups only become active at pH>10 and proteins at pH>8 (Bhatnagar et al., 2012) and their contributions in this study are not significant due to the pH values used.

The pH values in these assays were chosen due to the acid constant (pK<sub>a</sub>) of each group studied, since in pH values lower than the pK<sub>a</sub> of the groups, they become protonated, reducing the possibility of binding with positively charged ions (Rakshae et al., 2009). The pK<sub>a</sub> of carboxyl groups is in the range of 3 and 5; while the pK<sub>a</sub> of sulfonics is between 1 and 2.5 (Bhatnagar et al., 2012; Sheng et al., 2004). Table 1 presents adsorption of copper by the modified and blocked biomaterial.

Blocking of the two groups resulted in a sharp drop in adsorption capacity of copper ions, when compared to the capacity of the macrophyte that was not blocked (treated). However, even after sterification, at pH 4, the adsorption is mainly associated to the carboxylic groups that were not blocked. Some authors present good quantitative ratio between the carboxylic groups that were indeed sterified and the decrease in adsorption (Bhatnagar et al., 2012). On the other hand, at pH 2, as well as parts of the carboxylic groups having been sterified, the remaining is protonated and the resulting removal, that is 75% lower in modified biomass, is attributed to the sulfonic groups, which bind to the metals mainly at low pH values (Fourest and Volesky, 1996).

In the case of biomass which had the sulfonic groups blocked, it can be observed that the adsorption capacity was reduced in over 90%. This is an evidence of the existence of other groups which might adsorb the metals in small quantities, as well as the ionic exchange phenomenon, which has a small role in the adsorption capacity of Cu<sup>2+</sup> ions by the macrophyte and confirms the preference for the carboxylic groups in the binding with metals, especially at pH 4.5, the pH used in this study.

### 3.5. Bioadsorption kinetic of Cu<sup>2+</sup> and Pb<sup>2+</sup> ions

Fig. 5 presents the bioadsorption kinetics for Cu<sup>2+</sup> and Pb<sup>2+</sup> ions. It can be observed that the process is extremely fast, reaching equilibrium between 25 and 50 min for both ions. This means that, even for low concentration solutions, the resistance to mass transference is not high, different from what happens in processes such as chemical precipitation, for instance, which is extremely inefficient in low concentrations. The kinetic models of pseudo-first and pseudo-second order, as well as intra-particle diffusion, were adjusted to the experimental data obtained. The results for the first two models are presented in Fig. 5 and Table 2. Both models presented a good adjustment to the experimental data, with elevated determination coefficient value for the two metallic ions.

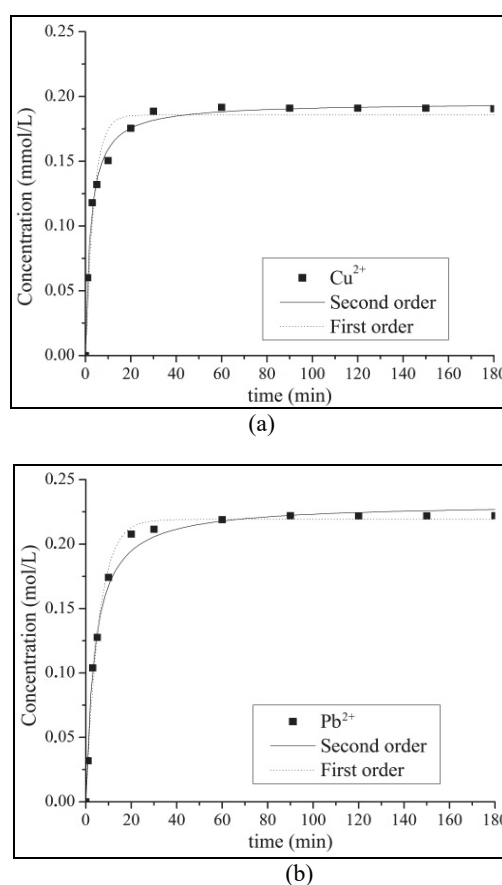


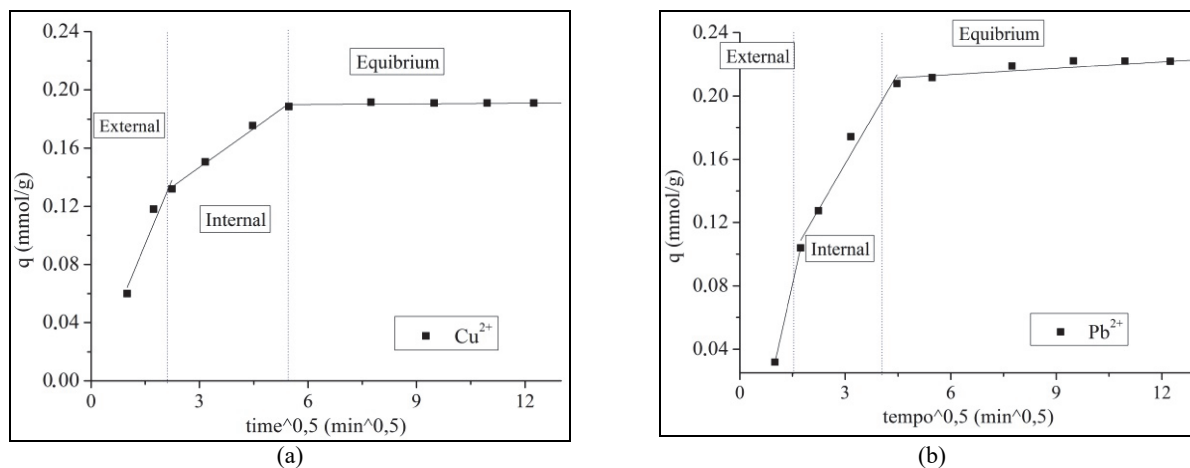
Fig. 5. Adjustment of pseudo-first and pseudo-second order kinetic models for (a) Cu<sup>2+</sup> and (b) Pb<sup>2+</sup> ions adsorbed in *A. pinnata*

Table 1. Result of copper ion adsorption after the blocking of functional groups

Macrophyte	Sterification of carboxylic groups (pH 4)		Sterification of carboxylic groups (pH 2)		Blocking of sulfonic groups (pH 2)	
	q (mmol g <sup>-1</sup> )	Decrease (%)	q (mmol g <sup>-1</sup> )	Decrease (%)	q (mmol g <sup>-1</sup> )	Decrease (%)
treated	0.191	51.33	0.191	75.31	0.191	92.27
blocked	0.093		0.047		0.015	

**Table 2.** Parameters for the pseudo-first and pseudo-second order models and adsorption capacity value experimentally obtained for Cu<sup>2+</sup> and Pb<sup>2+</sup>

Ions	Pseudo-first order model			Pseudo-second order model			Experimental value
	$q_1$ (mmolg <sup>-1</sup> )	$k_1$ (h <sup>-1</sup> )	$R^2$	$q_2$ (mmolg <sup>-1</sup> )	$k_2$ (gmmol <sup>-1</sup> min <sup>-1</sup> )	$R^2$	$q$ (mmolg <sup>-1</sup> )
Cu <sup>2+</sup>	0.186	0.283	0.971	0.196	2.291	0.995	0.191
Pb <sup>2+</sup>	0.219	0.178	0.991	0.231	1.158	0.992	0.222

**Fig. 6.** Intra-particle diffusion for the adsorption of (a) Cu<sup>2+</sup> and (b) Pb<sup>2+</sup> in *A. pinnata*

When the adsorption capacity values obtained by the pseudo-first ( $q_1$ ) and pseudo-second ( $q_2$ ) models are compared to the value experimentally obtained ( $q$ ), it can be noticed that the values for pseudo-first model are closer to the experimental data obtained for Pb<sup>2+</sup>, presenting a deviation of 1.37 % ( $q_1$  in relation to  $q$ ), thus making it the model that best describes the experimental data for this ion. However, the adsorption capacity value obtained by the adjustment of the pseudo-second order model ( $q_2$ ) was closest to the data obtained for Cu<sup>2+</sup>, presenting deviations of 2.55 % ( $q_2$  in relation to  $q$ ).

The mechanisms ruling the transference of mass during the adsorption may be simplified in stages. The diffusion in the external film is not limiting in the resistance to mass transfer when the agitation of the system is sufficiently high to avoid concentration gradients in the solution; the sorption is seen as an almost-instantaneous mechanism; thus, the resistance to mass transfer external to the particle and intra-particle are probably the phenomena controlling the process kinetic (Guibal et al., 1998). For Volesky (2001), the sorption reactions are quick and usually, this is not the stage that controls bioadsorption process rate. Intra-particle diffusion is usually the limiting stage in these processes and, therefore, the stage controlling the rate of the whole process.

According to Chen et al. (2003), when the adsorption capacity is plotted in relation to  $\text{time}^{0.5}$  (model proposed by Weber and Morris, 1962), it can be assumed that the behavior of the resulting curve will present three different stages: the first linear stage where a quick external diffusion takes place

(attributed to the diffusion on the external film); the second linear stage is a gradual adsorption where the intra-particle diffusion is the limiting factor; and the final stage of equilibrium, where the intra-particle diffusion decreases due to the small number of active sites available for adsorption. Fig. 6 presents the adjustment of the intra-particle diffusion model and shows the three stages predicted by this model.

When the adsorption is controlled by the intra-particle diffusion, with a linear regression in the intermediary portion (second stage), it follows that the inclination of the line is the intra-particle transport velocity constant ( $k_3$ ). The values of constant  $k_3$  (mmolg<sup>-1</sup>min<sup>-0.5</sup>) and determination coefficient ( $R^2$ ) for adsorption in *A. pinnata* were 0.018 and 0.99 for Cu<sup>2+</sup> ion, and 0.038 and 0.96 for Pb<sup>2+</sup> ion, respectively.

On the other hand, the line obtained from the linear regression in stage one (external diffusion) did not go through the origin in any of the cases presented. This deviation indicates that the intra-particle diffusion is not the only stage limiting the adsorption rate and that other complex mechanism might be simultaneously taking place (Jain, 2001).

### 3.6. Equilibrium assays

Fig. 7 shows the experimental adsorption isotherms obtained and the adjustment of Langmuir and Freundlich models to the experimental data at temperatures of 25°C and 45°C, for each metal studied. Higher temperature resulted in an increase in maximum adsorption capacity ( $q_{max}$ ) for both ions studied.



The parameters for maximum adsorption capacity ( $q_{max}$ ), the  $K$  constants, the determination coefficients and the  $R_L$  parameters are presented in Table 3. Since  $K$  is related to the binding energy between the adsorbent and the adsorbate, the differences found when the temperature varies is evidence of its influence in the interaction between the biomaterial and the ions studied. It can be seen by the determination coefficient ( $R^2$ ) that the model appropriately describes the data for the process. The values obtained for  $R_L$  were lower than one, and therefore, according to the definition by McCabe et al. (2001), all isotherms obtained are favourable.

The results obtained indicate that a greater energy associated to the binding between the metal and the adsorbent do not necessarily result in a greater quantity of metallic ions adsorbed, since the values of  $K$  found for lead ion are lower and this is the ion presenting the highest value for maximum adsorption capacity. Table 4 presents the calculated values for  $K_F$ ,  $n$  and  $n^{-1}$  from Freundlich's isotherm, which are related to the quantity of adsorption and the intensity of the binding, respectively. The higher the value of  $K_F$ , the better is the adsorption. However, this parameter is not the maximum

adsorption quantity, since Freundlich model does not predict the saturation of solid (Frimmel and Huber, 1996). A value of  $n < 1$  indicates that the intensity of removal is favorable in the concentration range studied; a value of  $n = 1$  indicates a linear relation; and for  $n > 1$ , the removal intensity is favorable in high concentrations (Frimmel and Huber, 1996; Treybal, 1988). Furthermore, according to McKay et al. (1979), for  $1/n$  values in the 2–10 range, the adsorption is appropriated.

Therefore, the results obtained in this work show that the adsorption process is promising for both ions studied. The parameter  $q_{max}$  obtained from Langmuir isotherm model is usually used in literature for comparing adsorption capacities for different adsorbents. Table 5 shows the values obtained in literature for several adsorbent materials and biomaterials in the adsorption of heavy metals. As it can be noticed, the adsorption capacity values of biomaterials are, in general, much higher than materials such as clay, activated carbon, and zeolites.

Furthermore, the *A. pinnata* presented significant  $q_{max}$  values, simplicity for usage and also, due to its availability and cost, it can be considered an attractive bioadsorbent for this process.

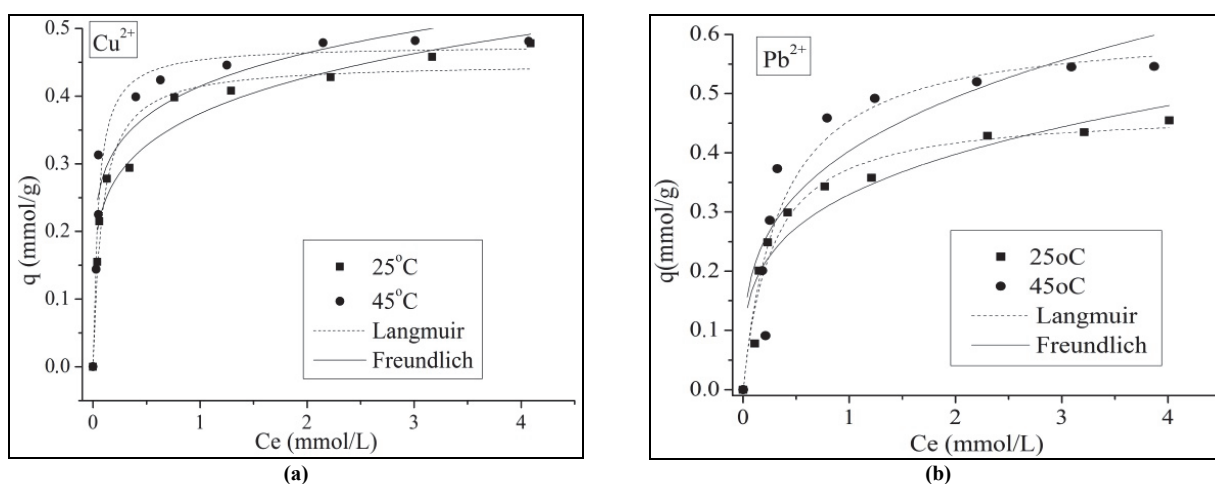


Fig. 7. Adjustment of adsorption isotherms according to the Langmuir model for (a)  $\text{Cu}^{2+}$  and (d)  $\text{Pb}^{2+}$  ions in the adsorption process in *A. pinnata*

Table 3. Parameters in the Langmuir model adjusted to the experimental data in the adsorption of  $\text{Cu}^{2+}$  and  $\text{Pb}^{2+}$  in pre-treated *A. pinnata* at temperatures 25 and 45°C, and pH 4.5

Ion	$q_{max} \text{ (mmol g}^{-1}\text{)}$		$K \text{ (Lmmol}^{-1}\text{)}$		$R^2$		$R_L$	
	25°C	45°C	25°C	45°C	25°C	45°C	25°C	45°C
$\text{Cu}^{2+}$	0.448	0.474	14.09	21.28	0.968	0.962	0.014	0.009
$\text{Pb}^{2+}$	0.472	0.614	3.76	2.84	0.965	0.910	0.051	0.066

Table 4. Parameters from the Freundlich model adjusted to the experimental data in the adsorption of  $\text{Cu}^{2+}$  and  $\text{Pb}^{2+}$  in pre-treated *A. pinnata* at temperatures 25 and 45°C, and pH 4.5

Ion	$K_F$		$n$		$n^{-1}$		$R^2$	
	25°C	45°C	25°C	45°C	25°C	45°C	25°C	45°C
$\text{Cu}^{2+}$	0.379	0.414	0.181	0.163	5.520	6.130	0.919	0.831
$\text{Pb}^{2+}$	0.329	0.403	0.271	0.291	3.690	3.420	0.856	0.735

**Table 5.** Ion adsorption capacity for different bioadsorbents

Adsorbent	Metallic Ion	$q_{max}$ (mmol/g)	Reference
Clay "slime-green"	Cu <sup>2+</sup>	0.06	Almeida Neto et al. (2011)
Activated carbon	Cd <sup>2+</sup> and Cd <sup>2+</sup>	0.068 and 0.051	Teker et al. (1999)
Clinoptilolite (Zeolite)	Cd <sup>2+</sup> and Pb <sup>2+</sup>	0.044 and 0.129	Sprynskyy et al. (2006)
Algae <i>N. zarnadini</i>	Cd <sup>2+</sup> , Ni <sup>2+</sup> and Zn <sup>2+</sup>	0.174; 0.275 and 0.533	Montazer-Rahmati et al. (2011)
Macrophyte <i>E. crassipes</i>	Cd <sup>2+</sup> and Zn <sup>2+</sup>	0.667 and 0.633	Módenes et al. (2011)
Algae <i>Sargassum fluitans</i>	Cd <sup>2+</sup> , Cu <sup>2+</sup> , Pb <sup>2+</sup> and Zn <sup>2+</sup>	1.15; 1.61; 1.65 and 0.81	Lee and Suh (2001)
Fungus <i>Rhizopus cohnii</i>	Cd <sup>2+</sup> , Ni <sup>2+</sup> , Pb <sup>2+</sup> and Zn <sup>2+</sup>	0.24; 0.32; 0.27 and 0.21	Fourest and Roux (1992)
Macrophyte <i>Azolla pinnata</i>	Cu <sup>2+</sup> and Pb <sup>2+</sup>	0.448 and 0.472	Present study

**Table 6.** Efficiencies in the adsorption-desorption-adsorption cycle and loss of mass during the desorption process of Cu<sup>2+</sup> and Pb<sup>2+</sup>

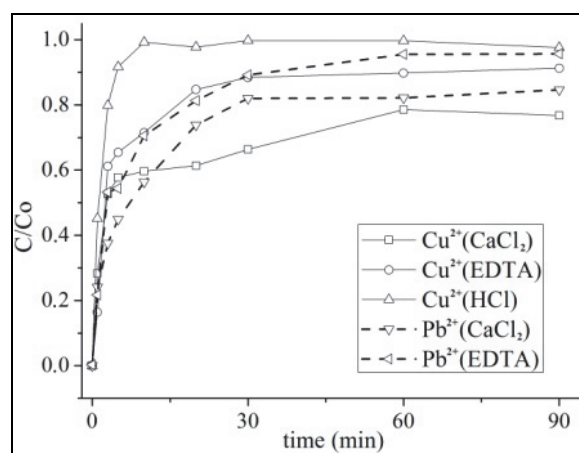
	Cu <sup>2+</sup>			Pb <sup>2+</sup>	
	CaCl <sub>2</sub>	EDTA	HCl	CaCl <sub>2</sub>	EDTA
Efficiency 1 <sup>st</sup> adsorption (%)	85.30	86.79	86.28	91.76	94.22
Efficiency desorption (%)	84.26	91.29	98.80	87.46	95.73
Efficiency 2 <sup>nd</sup> adsorption (%)	82.38	58.97	-	91.09	61.09
Loss of adsorption capacity (%)	3.42	32.05	-	3.20	35.16
Loss of mass (%)	6.92	16.38	-	4.93	11.93

### 3.7. Desorption in batches

In desorption in batches, the eluents HCl (0.1M), EDTA (0.05M) and CaCl<sub>2</sub> (0.5M) were evaluated. The results can be seen in Fig. 8, which presents the kinetic for this process. Many works in literature point out HCl as the most efficient eluent of heavy metals (Lee and Chang, 2011; Vijayaraghavan et al., 2012; Zhao et al., 1999). In the case of *A. pinnata* in this paper, despite the high value of copper desorption efficiency (98.8%), the material has become useless for later cycles and desorption of lead was not evaluated. Therefore, in this study, HCl did not present itself as a good eluent agent for this macrophyte.

Table 6 presents efficiency values in each stage of the adsorption-desorption-adsorption cycle, and it can be noticed that EDTA was more efficient in the elution of the two ions when compared to CaCl<sub>2</sub>. This might be due to the high value of the formation constant ( $K_f$ ) for Cu(II)-EDTA and Pb(II)-EDTA complexes ( $K_f = 5e10^{18}$  and  $3.85e10^{11}$  respectively at 25°C), which favors the formation of complexes (Dean, 1998; Martins et al., 2006). Nonetheless, the adsorption capacity of the biomass after desorption with EDTA was not sustained in the following cycle, with a decrease of over 30%, resulting in expressive loss of bioadsorbent mass. Therefore, this eluent is also not recommended for desorption of ions from *A. pinnata*.

The use of CaCl<sub>2</sub> does not interfere significantly in the 2nd adsorption nor results in expressive loss of mass. Moreover, the process was efficient and fast, reaching equilibrium in approximately 60 min. A fast process might increase the lifespan of the biomaterial and decrease the destruction of active sites (Lodeiro et al., 2006).

**Fig. 8.** Desorption kinetic for Cu<sup>2+</sup> and Pb<sup>2+</sup> ions using as eluents: HCl (0.1 M), CaCl<sub>2</sub> (0.5 M) and EDTA (0.05 M) with Co=0.5 mmolL<sup>-1</sup> and T=25°C

Comparing the elution efficiencies of ions, it can be observed that both for EDTA and CaCl<sub>2</sub>, the amount of lead ions desorbed is greater than copper ions, despite the copper ion presenting the lowest affinity by the macrophyte. Nonetheless, Pb<sup>2+</sup> presented the value of 3.78 Lmmol<sup>-1</sup> for the  $K$  constant in the Langmuir model, a lower value than that for Cu<sup>2+</sup> (11.90 Lmmol<sup>-1</sup>). The  $K$  constant indicates the binding energy, that is, it is related to the strength with which the ligands are bound (Shukla and Pai, 2005). Therefore, it can be concluded that the Cu<sup>2+</sup> ions are more strongly bound to the bioadsorbent, being more difficult to be removed in desorption and, thus, presenting a greater resistance to desorption when compared to the Pb<sup>2+</sup> ions.

#### 4. Conclusions

In this work, copper and lead uptake by *A. pinnata* was studied in order to evaluate biomass adsorption capacity as well as provide understanding of binding process. EDX and FTIR evidenced the disappearance of competing ions after adsorption suggesting that ionic exchange phenomenon might be one of the mechanisms occurring. Furthermore, analysis of functional groups showed carboxylic groups as the most active in the process.

Kinetic assays indicated that several mass transference stages limit the diffusion of ions and ( $q_{max}$ ) values obtained were satisfactory, mainly when compared to the non-biological adsorbent materials. Finally, desorption process using  $\text{CaCl}_2$  was efficient and viable, allowing the re-usage of the macrophyte.

#### Acknowledgements

The authors would like to acknowledge CNPq and FAPESP for the financial support.

#### References

Almeida Neto A.F., Vieira M.G.A., Silva M.G.C.da, (2012), Cu (II) adsorption on modified bentonitic clays: different isotherm behaviors in static and dynamic systems, *Materials Research*, **15**, 114-124.

Arora A., Saxena S., Sharma D.K., (2006), Tolerance and phytoaccumulation of Chromium by three *Azolla* species, *World Journal of Microbiology & Biotechnology*, **22**, 97-100.

Bharti S., Banerjee T.K., (2012), Phytoremediation of the coalmine effluent, *Ecotoxicology and Environmental Safety*, **81**, 36-42.

Bhatnagar A., Vilar V.J.P., Ferreira C., Botelho C.M.S., Boaventura R.A.R., (2012), Optimization of nickel biosorption by chemically modified brown macroalgae (*Pelvetia canaliculata*), *Chemical Engineering Journal*, **193**, 256-266.

Cardwell A.J., Hawker D.W., Greenway M., (2002), Metal accumulation in aquatic macrophytes from southeast Queensland, Australia, *Chemosphere*, **48**, 653-663.

Çelekli A., Yavuzatmaca M., Bozkurt H., (2010), An ecofriendly process: predictive modelling of copper adsorption from aqueous solution on *Spirulina platensis*, *Journal of Hazardous Materials*, **173**, 123-129.

Chen J.P., Yang L., (2005), Chemical modification of *Sargassum* sp. for prevention of organic leaching and enhancement of uptake during metal biosorption, *Industrial and Engineering Chemistry Research*, **44**, 9931-9942.

Chen J.P., Wu S., Chong K.-H., (2003), Surface modification of a granular activated carbon by citric acid for enhancement of copper adsorption, *Carbon*, **41**, 1979-1986.

Davis T.A., Volesky B., Vieira R.H.S.F., (2000), *Sargassum* seaweed as biosorbent for heavy metals, *Water Research*, **34**, 4270-4278.

Dean J.A., (1998), *Lange's Handbook of Chemistry*, McGraw-Hill, 15th Edition.

Doshi H., Ray A., Kothari I.L., (2007), Biosorption of cadmium by live and dead *Spirulina*: IR spectroscopic, kinetics, and SEM studies, *Current Microbiology*, **54**, 213-218.

Ferentinos L., Smith J., Valnzuela H., (2002), *Azolla*, *Sustainable Agriculture Green Manure Crops Aug*, SAGM-2, 1-3, On line at: <https://scholarspace.manoa.hawaii.edu/bitstream/10125/12732/1/SA-GM-2.pdf>.

Fourest E., Roux J.-C., (1992), Heavy metal biosorption by fungal mycelia by-products: mechanisms and influence on pH, *Applied Microbiology and Biotechnology*, **37**, 399-403.

Fourest E., Volesky B., (1996), Contribution of sulfonate groups and alginate to heavy metal biosorption by the dry biomass of *Sargassum fluitans*, *Environmental Science and Technology*, **30**, 277-282.

Frimmel F.H., Huber L., (1996), Influence of humic substances on the aquatic adsorption of heavy metals on defined mineral phases, *Environmental International*, **22**, 507-517.

Gardea-Torresdey J., Becker-Hapak M.K., Hosea J.M., Darnall D.W., (1990), Effect of chemical modification of algal carboxyl groups on metal ion binding, *Environmental Science and Technology*, **24**, 1372-1378.

Guibal E., Milot C., Tobin J.M., (1998), Metal-anion sorption by chitosan beads: equilibrium and kinetics studies, *Industrial and Engineering Chemical Research*, **37**, 1454-1463.

Guibal E., Roulph C., Cloirec P.L., (1992), Uranium biosorption by a filamentous fungus *Mucor miehei* pH effect on mechanisms and performances of uptake, *Water Research*, **26**, 1139-1145.

Guibaud G., Tixier N., Bouju A., Baudu M., (2003), Relation between extracellular polymers composition and its ability to complex Cd, Cu and Pb, *Chemosphere*, **52**, 1701-1710.

Gupta V.K., Rastogi A., (2008), Biosorption of lead from aqueous solution by green algae *Spirogyra* species: Kinetics and equilibrium studies, *Journal of Hazardous Materials*, **152**, 407-414.

Gupta V.K., Rastogi A., Nayak A., (2010), Biosorption of nickel onto treated alga (*Oedogonium hatei*): application of isotherm and kinetic models, *Journal Colloids and Interface Science*, **342**, 533-539.

Jachula J., Kolodynska D., Hubicki Z., (2016), Multifunctional resin diphenyl in adsorption of heavy metal complexes with methylglycinediacetic acid, *Environmental Engineering and Management Journal*, **15**, 2459-2468.

Jain C.K., (2001), Adsorption of zinc onto bed sediments of the River Ganga: Adsorption models and kinetics, *Hydrological Sciences Journal des Sciences Hydrologiques*, **46**, 416-434.

Jain C.K., Vasudevan P., Jha N.K., (1990), *Azolla pinnata* R. Br. and *Lemna minor* L. for removal of lead and zinc from polluted water, *Water Research*, **24**, 177-183.

Kratochvil D., Volesky B., (1998), Advances in the biosorption of heavy metals, *Trends in Biotechnology*, **16**, 291-300.

Kleinübing S.J., Silva E.A., Silva M.G.C.da, Guibal E., (2011), Equilibrium of Cu(II) and Ni(II) biosorption by marine alga *Sargassum filipendula* in a dynamic system: Competitiveness and selectivity, *Bioresource Technology*, **102**, 4610-4617.

Kleinübing S.J., Guibal E., Silva E.A., Silva M.G.C.da, (2012), Copper and nickel competitive biosorption simulation from single and binary system by *Sargassum filipendula*, *Chemical Engineering Journal*, **184**, 16-22.

- Lee Y.-C., Chang S.-P., (2011), The biosorption of heavy metals from aqueous solution by *Spirogyra* and *Cladophora* filamentous macroalgae, *Bioresource Technology*, **102**, 5297-5304.
- Lee H. S., Suh J.H., (2001), Interference of aluminum in heavy metal biosorption by seaweed biosorbent, *Korean Journal of Chemical Engineering*, **18**, 692-697.
- Lodeiro P., Herrero R., Sastre de Vicente M.E., (2006), Batch desorption studies and multiple sorption-regeneration cycles in a fixed-bed column for Cd(II) elimination by protonated *Sargassum muticum*, *Journal of Hazardous Materials B*, **137**, 1649-1655.
- Lumpkin T.A., Plucknett D.L., (1980), *Azolla*: Botany, physiology and use as a green manure, *Economic Botanic*, **34**, 111-153.
- Manciulea I., Bogatu C., Dumitrescu L., Draghici C., (2017), Cu<sup>2+</sup> removal from wastewaters by using compost as sorbent, *Environmental Engineering and Management Journal*, **16**, 779-792.
- Martins B.L., Cruz C.C.V., Luna A.S., Henriques C.A., (2006), Sorption and desorption of Pb<sup>2+</sup> ions by dead *Sargassum* sp. biomass, *Biochemical Engineering Journal*, **27**, 310-314.
- Mathlouthi M., Koenig J.L., (1987), Vibrational spectra of carbohydrates, *Advances in Carbohydrate Chemistry and Biochemistry*, **44**, 7-89.
- McCabe W.L., Smith J.C., Harriot P., (2001), *Unit Operations of Chemical Engineering*, 6th Edition, McGraw-Hill.
- McKay G., Otterburn M. S., Sweeney A.G., (1979), The removal of colour from effluent using various adsorbents – IV. Silica: Equilibrium and column studies, *Water Research*, **14**, 21-27.
- Módenes A.N., Espinoza-Quiñones F.R., Borba C.E., Trigueros D.E.G., Lavarda L., Abugderah M.M., Kroumov A.D., (2011), Adsorption of Zn(II) and Cd(II) ions in batch system by using the *Eichhornia crassipes*, *Water Science & Technology*, **64**, 1857-1863.
- Montazer-Rahmati M.M., Rabbani P., Abdolali A., Keshtkar A.R., (2011), Kinetics and equilibrium studies on biosorption of cadmium, lead and nickel ions from aqueous solutions by intact and chemically modified Brown algae, *Journal of Hazardous Materials*, **185**, 401-407.
- Puigdomenech I., (2004), HYDRA: Hydrochemical Equilibrium-Constant Database Software, Sweden, Royal Institute of Technology.
- Puranik P.R., Paknikar K.M., (1997), Biosorption of lead and zinc from solutions using *Streptovorticillium cinnamomeum* waste biomass, *Journal of Biotechnology*, **55**, 113-124.
- Rai P.K., (2007), Wastewater management through biomass of *Azolla pinnata*: An eco-sustainable approach, *Journal of the Human Environment*, **36**, 426-428.
- Rakshae R., Giahhi M., Pourahmad A., (2009), Studying effect of cell wall's carboxyl-carboxylate ratio change of *Lemna minor* to heavy metals from aqueous solution, *Journal of Hazardous Materials*, **163**, 165-173.
- Saygideger S., Gulnaz O., Istifli E. S., Yucel N., (2005), Adsorption of Cd(II), Cu(II) and Ni(II) ions by *Lemna minor* L.: Effect of physicochemical environment, *Journal of Hazardous Materials B*, **126**, 96-104.
- Selatnia A., Madani A., Bakhti M.Z., Kertous L., Mansouri Y., Yous Y., (2004), Biosorption of Ni<sup>2+</sup> from aqueous solution by a NaOH-treated bacterial dead *Streptomyces rimosus* biomass, *Minerals Engineering*, **17**, 903-911.
- Schimmel D., Fagnani K.C., Santos J.B.O. dos, Barros M.A.S.D., da Silva E.A., (2010), Adsorption of turquoise blue QG reactive dye on commercial activated carbon in batch reactor: kinetic and equilibrium studies, *Brazilian Journal of Chemical Engineering*, **27**, 289-298.
- Sheng P.X., Ting Y.-P., Chen J.P., Hong L., (2004), Sorption of lead, copper, cadmium, zinc and nickel by marine algal biomass: characterization of biosorptive capacity and investigation of mechanism, *Journal of Colloid and Interface Science*, **275**, 131-141.
- Shukla S.R., Pai S.R., (2005), Adsorption of Cu (II), Ni (II) and Zn(II) on modified jute fibers, *Bioresource Technology*, **96**, 1430-1438.
- Sprynskyy M., Buszewski B., Terzyk A.P., Namiesnik J., (2006), Study of the selection mechanism of heavy metal (Pb<sup>2+</sup>, Cu<sup>2+</sup>, Ni<sup>2+</sup> and Cd<sup>2+</sup>) adsorption on clinoptilolite, *Journal of Colloid and Interface Science*, **304**, 21-28.
- Teker M., Imamoglu M., Saltabas Ö., (1999), Adsorption of copper and cadmium ions by activated carbon from rice hulls, *Turkish Journal of Chemistry*, **23**, 185-191.
- Treybal R.E., (1988), *Mass-Transfer Operations*, 2nd Edition, McGraw-Hill.
- Vijayaraghavan K., Gupta S., Joshi U.M., (2012), Comparative assessment of Al(III) and Cu(II) biosorption onto *Turbinaria conoides* in single and binary systems, *Water Air Soil Pollution*, **223**, 2923-2931.
- Volesky B., (2001), Detoxification of metal-bearing effluents: biosorption for next century, *Hydrometallurgy*, **59**, 203-216.
- Wagner G.M., (1997), *Azolla* – A review of its biology and utilization, *The Botanical Review*, **63**, 1-26.
- Weber Jr.W.J., Morris J.C., (1962), *Advances in Water Pollution Research*, Pergamon Press, 231-266.
- Wilde E., Benemann J.R., (1993), Bioremoval of heavy metals by the use of microalgae, *Biotechnology Advances*, **11**, 781-812.
- Yoonaiwong W., Kaewsarn P., Reanprayoon P., (2011), Biosorption of lead and cadmium ions by non-living aquatic macrophyte, *Utricularia aurea*, *Sustainable Environmental Research*, **21**, 369-374.
- Zhao M., Duncan J.R., Van Hille R.P., (1999), Removal and recovery of zinc from solution and electroplanting effluent using *Azolla filiculoides*, *Water Research*, **33**, 1516-1522.